nature astronomy

ARTICLES

https://doi.org/10.1038/s41550-020-01276-x

Check for updates

An X-ray burst from a magnetar enlightening the mechanism of fast radio bursts

M. Tavani[1,2]✉, C. Casentini[1,3], A. Ursi[1], F. Verrecchia[4,5], A. Addis[6], L. A. Antonelli[5], A. Argan[1], G. Barbiellini[7,8], L. Baroncelli[6], G. Bernardi[9,10], G. Bianchi[9], A. Bulgarelli[6], P. Caraveo[11], M. Cardillo[1], P. W. Cattaneo[12], A. W. Chen[13], E. Costa[1], E. Del Monte[1], G. Di Cocco[6], G. Di Persio[1], I. Donnarumma[14], Y. Evangelista[1], M. Feroci[1], A. Ferrari[15,16], V. Fioretti[6], F. Fuschino[6], M. Galli[17], F. Gianotti[6], A. Giuliani[11], C. Labanti[6], F. Lazzarotto[1], P. Lipari[18,19], F. Longo[7,8], F. Lucarelli[4,5], A. Magro[20], M. Marisaldi[6,21], S. Mereghetti[11], E. Morelli[6], A. Morselli[3], G. Naldi[9], L. Pacciani[1], N. Parmiggiani[6], F. Paoletti[22], A. Pellizzoni[23], M. Perri[4,5], F. Perotti[11], G. Piano[1], P. Picozza[2,3], M. Pilia[23], C. Pittori[4,5], S. Puccetti[14], G. Pupillo[9], M. Rapisarda[11], A. Rappoldi[12], A. Rubini[1], G. Setti[9,24], P. Soffitta[1], M. Trifoglio[6], A. Trois[23], S. Vercellone[25], V. Vittorini[1], P. Giommi[4,26] and F. D'Amico[14]

Fast radio bursts (FRBs) are millisecond radio pulses originating from powerful enigmatic sources at extragalactic distances. Neutron stars with large magnetic fields (magnetars) have been considered as the sources powering the FRBs, but the connection requires further substantiation. Here we report the detection by the AGILE satellite on 28 April 2020 of an X-ray burst in temporal coincidence with a bright FRB-like radio burst from the Galactic magnetar SGR 1935+2154. The burst observed in the hard X-ray band (18–60 keV) lasted about 0.5 s, it is spectrally cut off above 80 keV and implies an isotropically emitted energy of about 10^{40} erg. This event demonstrates that a magnetar can produce X-ray bursts in coincidence with FRB-like radio bursts. It also suggests that FRBs associated with magnetars can emit X-ray bursts. We discuss SGR 1935+2154 in the context of FRBs with low–intermediate radio energies in the range 10^{38}–10^{40} erg. Magnetars with magnetic fields $B \approx 10^{15}$ G may power these FRBs, and new data on the search for X-ray emission from FRBs are presented. We constrain the bursting X-ray energy of the nearby FRB 180916 to be less than 10^{46} erg, smaller than that observed in giant flares from Galactic magnetars.

Fast radio bursts (FRBs) are coherent radio pulses in the gigahertz range typically originating at large (gigaparsec) distances[1,2]. The FRB energetics and the short durations imply powerful emission phenomena requiring compact sources (neutron stars or black holes)[3]. Strongly magnetized neutron stars (magnetars[4]) of the type similar to the X-ray flaring sources detected in our Galaxy have been considered as possible candidates of FRB sources or of a subset of them. However, the lack of simultaneous detection of radio bursts with any other emission from FRBs or from magnetars so far prevented further progress. The situation drastically changed with the recent detection on 28 April 2020 of a remarkable radio burst from the Galactic magnetar source SGR 1935+2154 (refs. [5,6]), emission that occurred simultaneously with the X-ray emission reported here.

Soft gamma-ray repeaters (SGRs) are Galactic compact sources occasionally becoming active in producing tens or hundreds of X-ray/hard X-ray bursts within weeks or months. They are believed to be neutron stars classified as magnetars[4] releasing energy because of instabilities originating from their magnetospheres. SGR 1935+2154 is a magnetar first detected by the Swift satellite in 2014[7] and possibly associated with the supernova remnant G57.2+0.8 at 12.5 kpc (ref. [8]). It rotates with a spin period $P = 3.24$ s, and it has a dipole magnetic field $B_m = 2 \times 10^{14}$ G deduced from its spindown properties[9]. The source recently started a period of X-ray bursting on 22 April 2020[10].

During routine operations in April 2020, the AGILE satellite[11] detected many tens of hard X-ray bursts originating from SGR 1935+2154. The satellite instrument is currently operating with the fully operational mini-calorimeter (MCAL) detector sensitive in the 400 keV–100 MeV, and with Super-AGILE (SA), anti-coincidence (AC) and gamma-ray imager (GRID) ratemeters (RMs) being sensitive in the energy bands 18–60 keV, 80–200 keV and 20 keV–1 MeV, respectively. Figure 1 shows a sample of a sequence of many X-ray bursts attributed to SGR 1935+2154 (a 'burst forest') detected by

[1]INAF-IAPS Roma, Rome, Italy. [2]Dipartimento di Fisica, Università di Roma Tor Vergata, Rome, Italy. [3]INFN Roma Tor Vergata, Rome, Italy. [4]ASI Space Science Data Center, SSDC-ASI, Rome, Italy. [5]INAF - Osservatorio Astronomico di Roma, Monte Porzio Catone, Italy. [6]INAF-IASF Bologna, Bologna, Italy. [7]Dipartimento Fisica, Università di Trieste, Trieste, Italy. [8]INFN Trieste, Trieste, Italy. [9]INAF-IRA, Bologna, Italy. [10]Department of Physics and Electronics, Rhodes University, Grahamstown, South Africa. [11]INAF-IASF Milano, Milan, Italy. [12]INFN Pavia, Pavia, Italy. [13]School of Physics, Wits University, Johannesburg, South Africa. [14]Agenzia Spaziale Italiana, Rome, Italy. [15]Dipartimento di Fisica, Università di Torino, Turin, Italy. [16]Consorzio Interuniversitario Fisica Spaziale (CIFS), Turin, Italy. [17]ENEA Bologna, Bologna, Italy. [18]INFN Roma 1, Rome, Italy. [19]Dipartimento Fisica, Università La Sapienza, Rome, Italy. [20]Institute of Space Sciences and Astronomy (ISSA), University of Malta, Msida, Malta. [21]Birkeland Centre for Space Science, Department of Physics and Technology, University of Bergen, Bergen, Norway. [22]East Windsor RSD, Hightstown, NJ, USA. [23]INAF - Osservatorio Astronomico Cagliari, Capoterra, Italy. [24]Dipartimento di Fisica e Astronomia, Università di Bologna, Bologna, Italy. [25]INAF Osservatorio Astronomico di Brera, Merate, Italy. [26]Institute for Advanced Study, Technische Universitaet Muenchen, Garching bei Munchen, Germany. ✉e-mail: marco.tavani@inaf.it

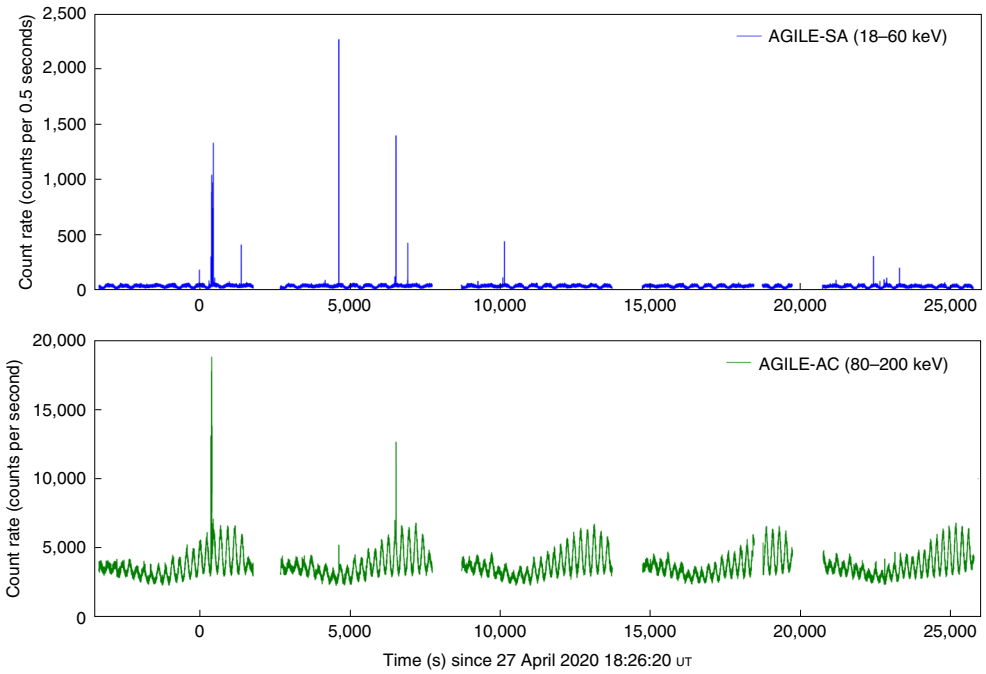

Fig. 1 | AGILE detection of the 'forest' of X-ray bursts from SGR 1935+2154. RM light curves of SA data in the 18–60 keV band (top) and AC data (80–200 keV) (bottom) including the time interval 27 April 2020 18:26 UT and 28 April 2020 01:45 UT. Several X-ray bursts from SGR 1935+2154 are clearly visible. The quasi-sinusoidal variations of the baseline light curves are caused by background variations induced by the satellite 7 min spinning. Gaps in the light curves are due to data flow interruptions because of passages over the South Atlantic Anomaly.

AGILE[12] during 7 h from 27 April 2020 18:31 UT until 28 April 2020 01:45 UT. These X-ray bursts have durations ranging from a fraction of a second to several seconds, and are quite bright, with fluences in the range of 10^{-5}–10^{-6} erg cm^{-2} (18–60 keV), implying isotropically emitted energies in the range 10^{41}–10^{42} erg (for a fiducial source distance $d = 10$ kpc assumed throughout this paper).

Among the several bursts detected on 28 April 2020, one X-ray burst is particularly relevant[13]: it was detected on 28 April 2020 at $T_0 = 14{:}34{:}24.000 \pm 0.256$ UT by the SA RM in temporal coincidence with the super-bright (double-peaked) radio pulse from SGR 1935+2154 revealed at 400–800 MHz by the Canadian Hydrogen Intensity Mapping Experiment (CHIME)/FRB[5] and at 1.4 GHz by the Survey for Transient Astronomical Radio Emission 2 (STARE2)[6]. The timing of the radio event provided by CHIME/FRB (topocentric arrival time at 400 MHz) agrees with that of the AGILE X-ray burst once the time difference of 8.6 s is taken into account as dispersive delay of radio waves along a path with dispersion measure DM = 332.8 pc cm^{-3} (ref. [5]). The CHIME/FRB radio fluence measurement at 400–800 MHz for the combined double-peaked event is 700 kJy ms (ref. [5]). For one of the peaks, STARE2 reports the very large fluence at 1.4 GHz of 1.5 MJy ms for a pulse of intrinsic width of 0.6 ms, corresponding to an isotropic energy release of $E_{\rm R,iso} = 2.2 \times 10^{35}\, {\rm d}^2_{\rm 10kpc}$ erg, where $\rm d_{10kpc}$ is the source distance in units of 10 kpc (ref. [6]). The CHIME and STARE2 fluences imply a spectral decrease at lower frequencies of the radio pulse detected by STARE2[5].

Compared with other X-ray bursts of the SGR 1935+2154 'forest', the X-ray burst coincident with the intense radio pulse is quite weak in the AGILE data as a consequence of intrinsic faintness of the event in the 18–60 keV band and geometry (event at 128° off-axis angle). Figure 2 shows the burst light curve in the 18–60 keV energy band. The event lasts no longer than 0.5 s and has a signal-to-noise ratio (SNR) of 3.8σ over the background; its false alarm rate is 3×10^{-3} Hz, and the post-trial significance is 2.9σ (Methods). No significant simultaneous detection is obtained from the data of the MCAL (lower energy threshold of 400 keV) and AC (lower threshold near 80 keV) detectors, indicating a burst with substantially reduced emission above 80 keV (Methods). This X-ray burst detected by AGILE is in temporal and spectral agreement with the simultaneous detection by several space instruments (Integral[14], Konus–Wind[15], Insight/Hard X-ray Modulation Telescope (HXMT)[16]). The fluence in the 18–60 keV band is 5×10^{-7} erg cm^{-2} corresponding to an isotropic equivalent emitted energy of $E_{\rm X,iso} = 8.1 \times 10^{39}\, {\rm d}^2_{\rm 10kpc}$ erg. The event lasts 0.5 s and has a spectral cutoff near 80 keV (also confirmed in refs. [14,15]) as obtained from the combined information of the AGILE detectors (Methods).

When compared with the properties of the radio burst, interesting features emerge. The ratio ξ between burst X-ray and radio energies is $\xi = E_{\rm X,iso}/E_{\rm R,iso} = 3 \times 10^4$, a value that is not dissimilar from what observed from impulsive mechanisms of particle acceleration and radiation in astrophysical shocks and unstable systems. What makes this X-ray event remarkable is its association with an FRB-like pulse of coherent radio emission lasting a fraction of a millisecond, a phenomenon never detected before from a magnetar system. Our detection shows that coherent radio emission with very large brightness temperature temporally coexists with an energy release of a short burst of X-rays up to ~100 keV. Locations of the radio and X-ray emissions can be the same or disjoint, leading to interesting possibilities as we discuss below.

Following the radio detection, SGR 1935+2154 was observed by our group at 408 MHz with the Northern Cross Telescope[17] from 30 April 2020 onwards initially with a daily cadence, which was relaxed in mid-June with observations every other day. The source was observed each day at transit, typically for 30 min. Data were acquired with a time resolution of 138 μs and frequency resolution of 12 kHz over a 16 MHz band; they were searched for bursts as large as 700 ms using a Heimdall-based pipeline in a DM range $0 < {\rm DM} < 1{,}000$ pc cm^{-3} (that is, ref. [18]). No radio burst detection was found above 7σ spectral fluence upper limits of ~25 Jy ms.

Interestingly, a 7σ detection of pulsed radio emission from SGR 1935+2154 with the 3.24 s period was obtained by the Northern

Cross on 30 May 2020[19]. This detection indicates that SGR 1935+2154 is an active magnetar capable of emitting transient pulsed emission about one month after the enhanced activity that led to the super-intense radio burst of 28 April 2020.

We can consider the energetics of the radio/X-ray burst from SGR 1935+2154 in the context of FRBs. Figure 3 shows the distribution of radio burst energies as a function of intrinsic time duration for all known FRB sources (see Methods for details on distances' determination). For comparison, we also add to the plot the $E_{R,iso}$ of SGR 1935+2154, enabling a sensible comparison between the energetics of FRBs and a magnetar. Remarkably, $E_{R,iso}$ of SGR 1935+2154 is of the same order of magnitude as the energies observed from the nearby FRB 180916 at the known distance of 150 Mpc (ref. [20]). The range of observed FRB radio energies is quite large (10^{36}–10^{42} erg) indicating that the FRB phenomenon implies extreme conditions compared with known magnetars. However, the radio burst of SGR 1935+2154 does not differ by more than two orders of magnitude compared with the lower end of the FRB population. If the average energy of the FRB radio bursts near 10^{38} erg is related to magnetar magnetic field dissipation, a larger factor of 10^2 in $E_{R,iso}$ magnitude can be accounted for by values of magnetic fields B_m larger than ~10 compared with that of the SGR 1935+2154 field, that is $B_m = 10^{15}$ G. Thus, the magnetar hypothesis for FRBs of radio energies near 10^{38} erg is plausible from the energetic point of view. We notice that FRB events at the lower end of the energy distribution are dominated by radio bursts detected from repeating FRBs, that is, from FRB sources that have been detected to emit several (sometimes tens or hundreds) radio pulses, usually in a sporadic pattern[21–23].

Regarding the X-ray emission, extrapolating from Fig. 3 and assuming the same ξ as for SGR 1935+2154, we would expect from FRBs emission of 1 s X-ray bursts related to radio bursts of energies near 10^{42} erg. Given the distances of known FRBs (Methods), fluxes from these X-ray bursts are too low to be detected by current space instruments. However, these are not the only type of X-ray burst that magnetars can produce. As shown by Galactic SGRs, much more intense X-ray bursts can occasionally be emitted (as reviewed in ref. [4]). Restricting our analysis to SGR 1935+2154, there might be different kinds of X-ray burst emitted by this magnetar. One type is made of the standard SGR bursts that can release 10^{40}–10^{43} erg of energy in 0.1–10 s duration bursts as detected during the 'burst forest' episode of Fig. 1. Even though one event is not enough to draw general conclusions, the X-ray burst associated with the intense coherent radio emission is of substantially lower intensity compared with the most luminous X-ray bursts of the 'forest type'. It is a fact that no X-ray bursts have been detected simultaneously with radio bursts from FRB 121102[24], and no other radio bursts were detected together with X-ray bursts from SGR 1935+2154[25].

These two types of burst can have different origins, either close to the magnetar surface (for example, refs. [26,27]) or relatively far from the magnetosphere (for example, refs. [28,29]). In addition to standard X-ray bursts (with no associated intense radio pulses) and events with radio bursts, SGRs are known to emit also rare 'giant' X-ray/gamma-ray flares of the type observed from SGR 1806–20 in 2004 that released more than 10^{46} erg in 200 ms up to megaelectronvolt energies[30,31] with no simultaneous radio emission[32]. Furthermore, active SGRs radiate long-timescale X-ray persistent emission about 100 times more intense than the quiescent state; in the case of SGR 1935+2154, the persistent X-ray luminosity during May 2020 is 8×10^{34} erg s^{-1} (ref. [33]).

If X-ray bursts are emitted by the FRBs at the lower end of the energy distribution of Fig. 3, interesting consequences follow. Magnetars associable to FRBs with low or intermediate radio energies most likely have magnetic fields near $B_m = 10^{15}$ G as indicated above. Magnetars with larger intrinsic magnetic fields, $B_m = 10^{16}$ G, have also been advocated for FRBs (for example, ref. [29]). We therefore might expect a broad range of X-ray burst fluxes depending on source distances, and detection of nearby FRBs by current X-ray monitoring instruments might be possible. Figure 4 shows the current upper limits obtained by AGILE for one of the most interesting repeating FRBs, the nearby FRB180916.J0158+65 (hereafter FRB 180916), which has the smallest redshift-determined distance of 150 Mpc (ref. [20]). This FRB source is not only repeating but also periodic with a period of 16.35 d (ref. [34]). The purple diamond in Fig. 4 shows the expected flux from an X-ray event similar to SGR 1935+2154 if put at the distance of 150 Mpc. Standard or 'giant' X-ray bursts from this magnetar would have larger fluxes from two to six orders of magnitude, respectively. Much harder is the detection of faint X-ray bursts of the type shown in Fig. 2 that requires a source substantially closer than FRB 180916.

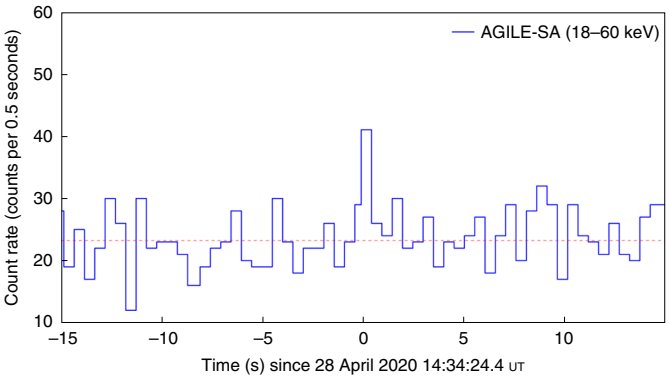

Fig. 2 | Detection of the X-ray burst in temporal coincidence with the very intense radio burst from SGR 1935+2154. The panel shows the light curve of the AGILE-SA RM with data in the energy range 18–60 keV displayed with 0.5 s binning.

In addition to the AGILE monitoring[35], we also carried out extensive observations of FRB 180916 at radio[18] and X-ray energies. Figure 5 shows the results of the Neil Gehrels Swift Observatory X-ray monitoring of FRB 180916 in the 0.3–10 keV range (3 February 2020 to 7 September 2020) that constrains both the flaring (shaded area of Fig. 4) and the persistent emissions. The cumulative Swift exposures are 37 ks in photon counting (PC) mode and 69 ks in windowed timing (WT) mode. The latter observing mode is more sensitive to short X-ray flaring. The resulting energy upper limit for X-ray bursts is less than 10^{46} erg for 1 s durations, that is, smaller than that of the giant flares from Galactic magnetars. The average luminosity of the persistent emission is constrained to be less than 10^{41} erg s^{-1}. Chandra observations in December 2019 obtained a lower value (2×10^{40} erg s^{-1})[36]. Given the peculiar radio burst repetition pattern of FRB 180916, these limits sensibly constrain physical interactions within the system (for example, refs. [37,38]).

Another source of interest is FRB 181030, which fares the smallest observed DM among the FRBs[23]. Once the Galactic and possible host-galaxy contributions are subtracted, the excess DM and resulting distance may be even less than those of FRB 180916[39]. It is then possible to detect X-ray bursts from this source by future monitoring.

It is uncertain whether a single or different types of compact object are related to the FRB phenomenon (for example, refs. [3,40]). We made the case of a closeness in energetics and overall phenomenology between SGR 1935+2154 and nearby FRBs. Whether this connection applies to the rest of the FRB population is uncertain. Figure 3 shows the energy of radio bursts of all FRBs (repeating and non-repeating ones) compared with the radio burst from SGR 1935+2154. The challenge of explaining six orders of magnitude of radio emission by models involving only magnetars is severe. More than one type of compact source might be involved[40]. Beaming and/or plasma lensing[41] are possible features of the emission that can alleviate many if not all of these issues. To provide a useful

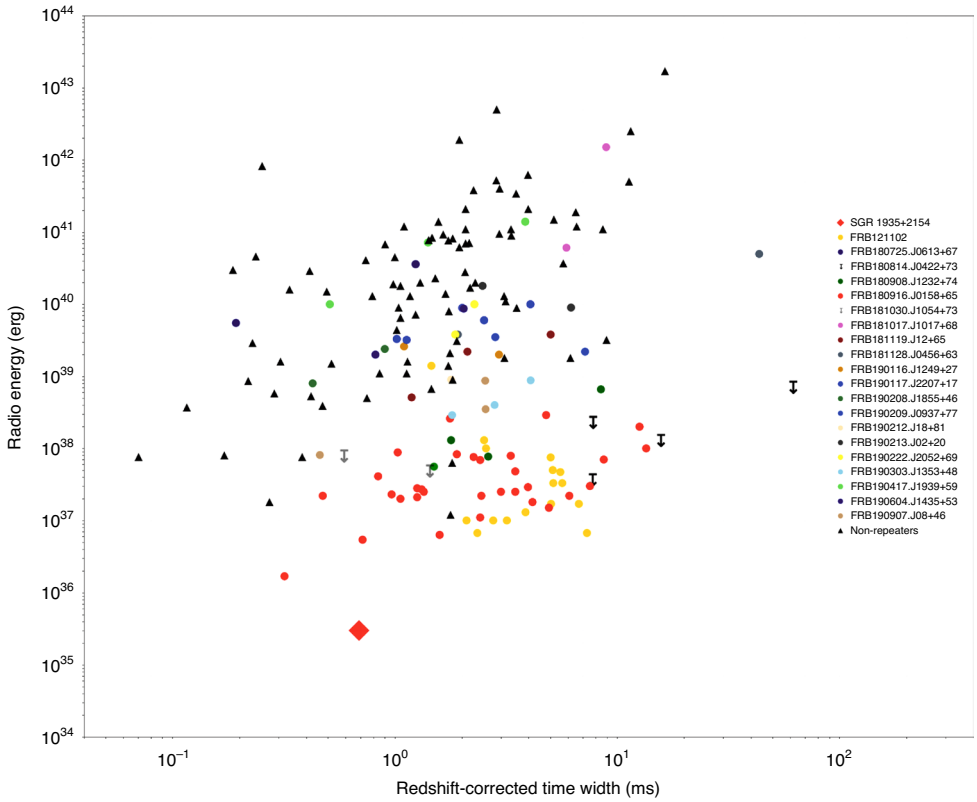

Fig. 3 | Isotropically emitted energies of radio bursts detected from FRBs versus their redshift-corrected intrinsic time widths of their emission. FRB radio data (typically in the 400 MHz–1.5 GHz band) and DM information are from ref. [2]. Black triangles are for non-repeating FRBs and coloured marks are for repeating FRBs. The red diamond marks the observed energy at 1.4 GHz and width of the very intense radio burst from SGR 1935+2154[6]. The red circles are the measurements of the periodic-repeating FRB 180916[2,20,23]. The distance of this source is 150 Mpc (ref. [20]). Distances of other FRBs have been derived from their intergalactic dispersion measure $DM_{(IM)}$ once the Galactic disk contribution has been subtracted from the total DM together with the Galactic halo and host-galaxy contributions (these latter values have been assumed to be equal to $DM_{(HALO)} + DM_{(HOST)} = 50 + 50 = 100\ pc\ cm^{-3}$, in good agreement with measurements of FRBs of known distances (Methods). Downward arrows indicate upper limits because of source distance uncertainty.

contribution to the energetics problem, the beaming and lensing factors b and l should be $b, l \leq 10^{-2}$. All quantities considered above for FRBs should be multiplied by the factors b and l to obtain their intrinsic values. If this correction were applied to the FRB energies of Fig. 3, the SGR 1935+2154 radio burst energy (assumed isotropically emitted) would fit those of nearby FRBs. More data are necessary to resolve this important issue.

The detection of X-rays simultaneous with the very bright radio burst from SGR 1935+2154 is relevant to make progress in understanding the physical mechanism of FRBs. X-ray bursts of SGRs are believed to be emitted by magnetar events near the magnetosphere involving magnetic field re-arrangements and Alfven wave emission and consequent particle heating (for example, ref. [42]). The location of the X-ray burst from SGR 1935+2154 associated with the very intense radio pulse is uncertain; the temporal coincidence with the radio burst is indicative of space closeness of the two emissions.

Modelling of FRB radio bursts has focused on coherent plasma radiation processes; a possible mechanism is electron cyclotron maser emission[43] in the context of relativistic shocks of magnetar outflows (for example, refs. [28,38,44]). Radiation in the gigahertz range can be emitted with FRB characteristics as a shock precursor of a relativistic fluid interacts with an upstream magnetized environment providing target material for decelerating the outflow. However, the cyclotron maser mechanism is intrinsically narrow band, with $\Delta\omega/\omega$ equal to a few, where ω is the emitted frequency, and no X-rays are expected by the precursor itself[44]. It is interesting to note that perpendicular shocks of the type believed to apply to pulsars and FRB systems do not produce power-law tails in purely electron–positron outflows in the absence of ions[43]. Rather, they lead to energy randomization as a consequence of cyclotron emission producing downstream quasithermal particle distributions. These types of shock therefore do not develop a full-blown non-thermal acceleration with power-law distributions to large energies[43]. Therefore, quasithermal electron–positron spectra may co-exist downstream with a temporary precursor propagating perpendicularly to the local magnetic field. In principle, an upstream-generated coherent radio pulse can co-exist with incoherent X-ray emission generated downstream.

Alternatively, the radio/X-ray emission site is close to the magnetar magnetosphere (for example, ref. [27]). In this case, the X-ray emission should resemble that of standard bursts, and radio emission can result from curvature radiation within a coherence length compatible with the magnetar geometry[27,45]. However, the coexistence of the multiple radiation processes considered so far, and the simultaneity of X-ray and radio emissions may be challenging for the models so far proposed. In any case, submillisecond X-ray and radio time resolutions are necessary to properly study the emission.

We conclude stating that low–medium intensity FRBs have observed radio bursts and deduced physical parameters not dissimilar from SGR 1935+2154; magnetars with magnetic fields in the range 10^{15}–10^{16} G can be the underlying sources, and X-ray observations may reveal soon X-ray bursting activity of nearby FRBs. Magnetars can be considered as strong candidates for explaining low–medium intensity FRBs; whether magnetar-driven processes

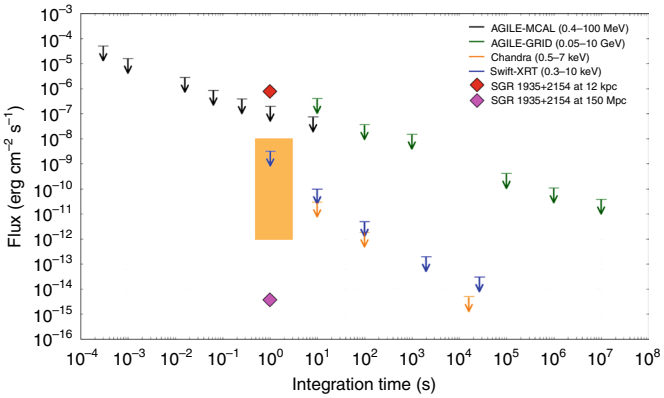

Fig. 4 | High-energy (X-ray and gamma-ray) 3σ flux upper limits as a function of integration timescales of observations obtained by AGILE, Swift and Chandra satellites in monitoring the nearby repeating FRB 180916. Data refer to different detectors of different satellites (AGILE[35,39], Swift[35] and Chandra[36]) in the energy ranges specified in the figure inset. We re-evaluated the upper limits of the Swift and Chandra instruments for integration timescales less than 10^3 s. We also display the flux of the 28 April 2020 X-ray burst from SGR 1935+2154 (red diamond) and for the same source at a 150 Mpc distance (purple diamond). Extrapolations of Swift and Chandra upper limits to 1 s integrations are obtained depending on observation modes. The shaded region in orange shows the flux range for possible X-ray outbursts from nearby magnetars associated with FRBs. A closer FRB source of a type similar to FRB 180916 and capable of producing X-ray bursts 10^3–10^4 times more luminous than the type-1 burst from SGR 1935+2154 might be detectable by future X-ray monitoring instruments. Upper limits shown here are applicable also to other FRBs; for example, for FRB 121102, X-ray fluence upper limits for single bursts of 1 s integration at the time of radio bursts are 2×10^{-10} erg cm^{-2} for observations simultaneous with XMM-Newton and 5×10^{-10} erg cm^{-2} for Chandra corresponding to energies 3×10^{46} erg and 6×10^{46} erg at the luminosity distance of FRB 121102, respectively[24].

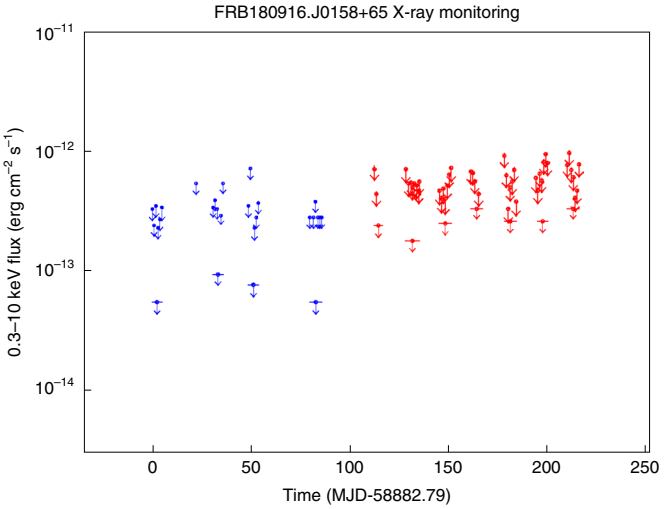

Fig. 5 | X-ray monitoring by Swift-XRT of the nearby repeating FRB 180916 (3 February 2020 to 7 September 2020) during its five-day active time intervals of expected radio bursting based on periodicity. Small arrows indicate flux upper limits in the range 0.3–10 keV obtained for XRT pointings lasting 1–2 ks. The lower value upper limits are the results of the sums of the individual pointings for different active time windows. Blue and red data refer to PC and WT observing modes, respectively. The cumulative exposures are 37 ks (PC) and 69 ks (WT). Updated data is from ref. [35].

can explain the bulk of FRBs is an open question that awaits more observations for its resolution.

Methods

AGILE scientific RMs. Data acquired by all AGILE detectors (that is, GRID, MCAL, SA and AC) are continuously collected and recorded in telemetry, and used to build broadband energy spectra in different energy ranges. The GRID, MCAL and AC RM data are acquired with a 1.024 s time resolution, whereas the SA RM data are acquired with a 0.512 s time resolution. In particular, the SA RMs acquire data in three energy channels (18–25 keV, 25–40 keV and 40–60 keV), which allows to carry out a three-channel spectral analysis for the detected events.

The RM data provide a continuous monitoring of the hard X-ray and gamma-ray background, allowing the investigation of its modulation in time and space through orbital phases. So far, the AGILE RMs have clearly detected a large number of high-energy transients, such as GRBs, SGRs and solar flares.

The AGILE scientific RMs are routinely calibrated, using GRBs reported by the Inter-Planetary Network, and used to compare the count rate and spectra acquired in the different energy bands with those provided for the same events by other space missions.

Direct and indirect spectral information from the AGILE detectors. For photon energies less than or near 1 MeV, the combination of AGILE detectors can obtain direct and indirect spectral information. Photon-by-photon acquisition by the SA and MCAL detectors provides spectra with energy resolution near 20–30% in the energy range 20–60 keV and 400 keV–100 MeV, respectively[11]. This information is available from SA data for events occurring in its 1sr field of view, or from MCAL data for omnidirectional incident directions. In addition, information is obtained from the top and four lateral sides of the AC system in the range 80–200 keV. Typically, GRBs detected by AGILE have complementary information from the AC, SA and MCAL detectors. Even for off-axis events, sufficiently intense bursts are detected from 20 keV up to MeV energies and above for typical band-like spectra extending up to MeV energies.

The SA detection efficiency strongly varies with the off-axis angle θ under which a given source is observed. A calibration of the SA RMs providing information on the response of the detector to different spectra and for different off-axis angles is routinely carried out by studying GRBs detected by SA and reported by other space missions.

The 28 April 2020 event detected by AGILE in coincidence with the strong radio pulse from SGR 1935+2154 was quite weak, observed under an off-axis of 120°, and not detected by MCAL. The consequence is spectral information based on only SA RMs and the absence of AC and MCAL signals.

For what concerns this event, we performed a calibration of the SA RMs, using the multiple events emitted by SGR 1935+2154 during the so-called burst forest. As this bursting activity lasted hundreds of seconds, SA observed these events under different off-axis angles during its spinning revolutions. This set of data allows us to study how a typical SGR spectrum (that is, a cutoff power law) is detected under various off-angles θ by the SA ratemeters, and how the detector efficiency is affected by the satellite spinning.

By adopting the almost on-axis bursts of the forest as a reference for the SA maximum efficiency, we evaluated how the response of the SA RMs varies within a range of off-axis angles. In particular, we focused on the events observed under $\theta \approx 120°$, which are typically detected with a flux reduction near 90%.

Despite the limited number of counts, a spectral analysis based on the three SM RM energy channels that takes into consideration the flux reduction at $\theta \approx 120°$ resulted in a spectral slope consistent with a cutoff power-law model for the flux $F = E^{-\alpha}\exp(-E(2-\alpha)/E_p)$ with photon index $\alpha = 0.52$ (−0.50, +0.57) and $E_p = 82$ keV (−9, +12) as reported by Konus–Wind[46].

Statistical significance of the X-ray burst from SGR 1935+2154 on 28 April 2020. The hard X-ray burst detected by the AGILE-SA RM on 28 April 2020 at $T_0 = 14{:}34{:}24.400 \pm 0.245$ s UT has an SNR of ~3.8 above a background rate of 45 Hz (in the 18–60 keV energy range). We estimated the occurrence of events with a SNR ≥ 3.8 in the AGILE-SA RMs, within ±2.5 ks around the T_0, and obtained a false alarm rate, FAR = 3×10^{-3} Hz.

Our signal occurs within ±0.25 s from the X-ray event detected by INTEGRAL/IBAS[14], Konus–Wind[15] and Insight-HXMT[16], compatible with the de-dispersed arrival topocentric time of the CHIME/FRB radio detection[5], at infinite frequency.

It is important to determine the false alarm probability (FAP) of a simultaneous occurrence of this event: this value strongly depends on the SNR, the FAR, the time interval between the nominal radio signal, and the X-ray burst, the bin width and the search window adopted for the search. We use the formula[47]

$$\mathrm{FAP} = \mathrm{FAR} \times \delta t \times \left[1 + \ln\left(\frac{\Delta t}{t_{\mathrm{bin}}}\right)\right]$$

Adopting the values, FAR = 0.003 Hz, a time distance $\delta t = 0.25$ s, a search window $\Delta t = 30$ s and a bin width $t_{\mathrm{bin}} = 0.5$, we obtain a post-trial probability $P = 0.0039 = 2.9\sigma$.

Table 1 | Assumptions and the resulting redshifts

Source	Ref.	DM (pc cm^{-3})	$DM_{(GAL)}$ (pc cm^{-3})	$DM_{(IG)}$ [a] (pc cm^{-3})	$DM_{(IG)}$ [b] (pc cm^{-3})	z_{est} [a]	z_{obs} [b]
FRB 121102	54	558.1 ± 3.3	188	270	171	0.300	0.19
FRB 180916	20	348.8 ± 0.1	199	50	31	0.056	0.034
FRB 180924	55	361.42 ± 0.06	40	221	289	0.246	0.321
FRB 181112	56	589.27 ± 0.03	42	447	432	0.490	0.48
FRB 190102	46	363.0 ± 0.3	40	224	262	0.249	0.291
FRB 190523	57	760.8 ± 0.6	37	624	594	0.690	0.66
FRB 190608	46	338.0 ± 0.5	40	199	106	0.221	0.1178
FRB 190611	46	321.0 ± 0.2	40	181	340	0.201	0.378[c]
FRB 190711	46	593.0 ± 0.4	40	453	470	0.503	0.522

In Fig. 3 we used for all FRBs the observed redshifts z_{obs} from the quoted references in this table. [a]Values of $DM_{(IG)}$ and estimated redshifts z_{est} obtained with the assumption $DM_{(HALO)} + DM_{(HOST)} = 100$ pc cm^{-3}. [b]Values of $DM_{(IG)}$ based on the measured redshifts z_{obs} of spatially coincident galaxies. The corresponding values of $DM_{(HALO)}$ and $DM_{(HOST)}$ are discussed in the reference papers. [c]This redshift is reported in ref. [46]; however, its consequent $DM_{(IG)}$ is larger than the total DM, and therefore the association of FRB 190611 with the proposed host galaxy is dubious.

Swift X-ray observations of FRB 180916. We are carrying out an observation campaign of FRB 180916 with the Neil Gehrels Swift Observatory (Swift) summarized in Fig. 5. The first set of Swift's X-ray Telescope (XRT) observations, until 29 April 2020, were taken in the PC readout mode; for observations carried out at later times, until 7 September 2020, the WT readout mode was used.

The Swift-XRT WT mode, used for bright sources with flux higher than a few mCrab, is obtained with a CCD (charge-coupled device) continuous clocking and the compression of ten consecutive rows in one single row along the detector y direction, followed by the readout of the central 200 columns of the CCD. This mode, with respect to the PC one, is characterized by a higher background and one-dimensional spatial resolution (along the detector x axis), but it substantially reduced instrumental pile-up for count rates up to ~200 counts per second. Also, the WT mode has a minimum temporal resolution of ~2 ms and therefore is well suited for the detection of short flares. The PC mode, while more sensitive for the detection of persistent emission from faint sources and capable of spatial two-dimensional information, has a much larger temporal resolution (~2.5 s) and moreover is significantly affected by pile-up for count rates larger than ~0.5 counts per second (~2×10^{-11} erg cm^{-2} s^{-1}). A detailed description of the Swift-XRT readout modes is given in ref. [48].

The Swift-XRT event files, both PC and WT modes, were calibrated and cleaned with standard filtering criteria with the xrtpipeline task (in the XRTDAS v.3.5.0 included in HEAsoft v6.27.1) using the calibration files available from the Swift-XRT CALDB (version 20200724). Events for the spectral analysis were selected within a circle of 20 pixel (~47 arcsec) radius, which encloses about 90% of the point spread function, centred at the source position. The background was extracted from a nearby circular region of 20 pixel radius. The search for X-ray flares has been carried out extracting the light curves with different temporal bins (10, 100 ms and 1 s) and evaluating the bin counts distribution to select those at $\geq 3\sigma$. No detections have been found.

We then evaluated the 3σ upper limit for each observation and then on the sum of all observations acquired during an activity cycle. Count rates were converted to 0.3–10 keV fluxes assuming an absorbed power-law spectral model with photon index 2.0 and hydrogen equivalent column density $N_H = 4.3 \times 10^{21}$ cm^{-2}.

FRB distances and intrinsic temporal widths. We use data on all FRBs observed so far through the FRBCAT catalogue[2,49], and the CHIME/FRB experiment online catalogue (available at the web pages https://www.frbcat.org and https://www.chime-frb.ca), with modifications for updated information.

We evaluate the FRB distances starting from the catalogued DM values. We considered four different contributors to the estimated DM: Galactic (Milky Way disk, $DM_{(GAL)}$), Galactic halo (Milky Way halo, $DM_{(HALO)}$), intergalactic, $DM_{(IG)}$ and host galaxy, $DM_{(HOST)}$. The $DM_{(GAL)}$ value was obtained from the catalogues. From the literature, we find $DM_{(HALO)}$ to be in the range 50–80 pc cm^{-3} (ref. [50]). As in our galaxy, we have a disk and a halo contribution also for the host galaxy. We sum the effects of these two contributions into a single value. In reasonable agreement with the FRB 180916 localization[20], we assume that $DM_{(HALO)} + DM_{(HOST)} = 100$ pc cm^{-3} for every FRB source with the exception of a few FRBs for which the resulting value of $DM_{(IG)}$ is negative. In these few cases, we adopt different values for $DM_{(HALO)} + DM_{(HOST)}$. We then estimate $DM_{(IG)}$ by subtracting Galactic and host contributions from the total value: $DM_{(IG)} = DM - DM_{(GAL)} - DM_{(HALO)} - DM_{(HOST)}$. Once $DM_{(IG)}$ is obtained, the FRB source distance is calculated using the relation $DM_{(IG)} = 900\,z$ pc cm^{-3} (ref. [51]). The resulting redshift value (z) is then used to estimate the distance following the cosmology as in ref. [51]. The same value of the redshift is also obtained for determining the intrinsic temporal widths of the FRB radio bursts, $\Delta t_{true} = \Delta t_{obs}/(1+z)$, where t_{true} is the true time after taking into account the redshift delay, and t_{obs} is the observed time.

It is important to test this procedure for a few critical FRBs of intrinsically small DM. A test case is FRB 180916, which has a total DM of about 350 pc cm^{-3} (refs. [1,23]). This value is expected to be the sum of $DM_{(GAL)}$, $DM_{(HALO)}$, $DM_{(HOST)}$ and $DM_{(IG)}$, which includes both the intergalactic contribution and that of the host galaxy. $DM_{(GAL)}$ is determined, following ref. [52], to be near 200 pc cm^{-3} (ref. [2]). We assume a value of 50 pc cm^{-3} for the halo component, $DM_{(HALO)}$. By subtracting $DM_{(GAL)}$ and $DM_{(HALO)}$ from the total DM, we are left with $DM_{excess} \approx 100$ pc cm^{-3}, to be divided between $DM_{(IG)}$ and $DM_{(HOST)}$. A redshift of $z = 0.0337$ corresponds to the measured distance of FRB 180916 (150 Mpc)[20]. For such a value of z, following the relation $DM_{(IG)}$–z, reported in ref. [51], we obtain $DM_{(IG)} \approx 31$ pc cm^{-3}. So, after the subtraction of $DM_{(IG)}$ from the excess 100 pc cm^{-3}, we are left with a value of $DM_{(HOST)}$ of the host galaxy around 69 pc cm^{-3}. We therefore determine that, despite uncertainties on the single components, the overall adopted value for the sum of $DM_{(HALO)}$ and $DM_{(HOST)}$ totalling ~100 pc cm^{-3} may be reasonable, and the uncertainties on the $DM_{(IG)}$ may be of the order of several tens of pc cm^{-3}.

Let us consider a case for which this procedure fails. The values for FRB 181030 are even smaller than in the previous case; if we adopted $DM_{(HALO)} + DM_{(HOST)} = 100$ pc cm^{-3} we would obtain a negative value of $DM_{(IG)}$ from a total value DM = 103.5 pc cm^{-3} and a Galactic plane contribution estimated to be $DM_{(GAL)} = 30$ pc cm^{-3} (ref. [23]). In this case, we adopt $DM_{(HALO)} + DM_{(HOST)} = 60$ pc cm^{-3}, which leads to $DM_{(IG)} = 13.5$ pc cm^{-3}, corresponding to $z \approx 0.015$ (around 65 Mpc). Clearly this value is uncertain and can be considered as an upper limit to the true distance of FRB 181030.

To evaluate the uncertainties in the determination of the $DM_{(IG)}$, we have checked the redshift values obtained by our method with the known redshifts determined for five FRBs. Table 1 summarizes the assumptions and the resulting redshifts obtained here; this table also shows the assumptions and the measured redshifts of the five FRBs as presented in the literature[20,53–57]. Our method based on the assumption $DM_{(HALO)} + DM_{(HOST)} = 100$ pc cm^{-3} provides values closer to the measured ones within a few percent for FRB 181112 and FRB 190523. Specific Milky Way halo plus host-galaxy contributions may be different from our general assumption. A noticeable case is FRB 180924 for which the measured host-galaxy redshift of $z = 0.321$ (ref. [54]) corresponds to a $DM_{(IG)} = 288$ pc cm^{-3} against our deduced value of 221 pc cm^{-3}. The corresponding redshifts differ by 30% as a consequence of a value of $DM_{(HALO)} + DM_{(HOST)}$ anomalously smaller than 100 pc cm^{-3}. The opposite case is provided by FRB 121102. We mark with arrow upper limits in Fig. 3 those few FRB events from sources with an apparent negative $DM_{(IG)}$ according to our procedure. For these FRBs, we adopt the measured distance of FRB 180916 (150 Mpc) as the distance upper limit for the energy determination.

We conclude that, despite the uncertainties on the individual contributions for $DM_{(HALO)}$ and $DM_{(HOST)}$ and source-specific peculiarities, the overall energy determinations of Fig. 3 are reasonable within factors of order two to four.

FRB radio energy estimates. Once the values of the distances are known for the individual FRBs, we proceed to the estimates of the energies of the radio bursts under the assumption of isotropic emission (for example, ref. [3]) taking into account the frequency range specific of each FRB. From our analysis, energy determinations are uncertain within factors of two to four.

Data availability

The data used in this investigation are available on demand at the helpdesk of the AGILE website: https://agile.ssdc.asi.it. The data that support the plots within this paper are available from the corresponding author.

Received: 18 May 2020; Accepted: 12 November 2020;
Published online: 18 February 2021

References

1. Lorimer, D. R., Bailes, M., McLaughlin, M. A., Narkevic, D. J. & Crawford, F. A. A bright millisecond radio burst of extragalactic origin. *Science* **318**, 777–780 (2007).
2. Petroff, E., Hessels, J. W. & Lorimer, D. R. Fast radio bursts. *Astron. Astrophys. Rev.* **27**, 4 (2019).
3. Cordes, J. M. & Chatterjeee, S. Fast radio bursts: an extragalactic enigma. *Annu. Rev. Astron. Astrophys.* **57**, 417–465 (2019).
4. Kaspi, V. & Beloborodov, A. M. Magnetars. *Annu. Rev. Astron. Astrophys.* **55**, 261–301 (2017).
5. Scholz, et al. A bright millisecond-timescale radio burst from the direction of the Galactic magnetar SGR 1935+2154. *Astron. Telegr.* 13681 (2020).
6. Bochenek, C. et al. Independent detection of the radio burst reported in ATel #13681 with STARE2. *Astron. Telegr.* 13684 (2020).
7. Stamatikos, M., Malesani, D., Page, K. L. & Sakamoto, T. GRB 140705A: swift detection of a short burst. *GRB Coord. Netw.* 16520 (2014).
8. Kothes, R., Sun, X., Gaensler, B. & Reich, W. A radio continuum and polarization study of SNR G57.2+0.8 associated with magnetar SGR 1935+2154. *Astrophys. J.* **852**, 54 (2018).
9. Israel, G. et al. The discovery, monitoring and environment of SGR J1935+2154. *Mon. Not. R. Astron. Soc.* **457**, 3448–3456 (2016).
10. Hurley, K. et al. IPN triangulation of a bright burst from SGR 1935+2154. *GRB Coord. Netw.* 27625 (2020).
11. Tavani, M. et al. The AGILE mission. *Astron. Astrophys.* **502**, 995–1013 (2009).
12. Ursi, A. et al. AGILE detection of a short and hard X-ray burst possibly related to SGR 1935+2154. *GRB Coord. Netw.* 27687 (2020).
13. Tavani, M. et al. AGILE detection of a hard X-ray burst in temporal coincidence with a radio burst from SGR 1935+2154. *Astron. Telegr.* 13686 (2020).
14. Mereghetti, S. et al. INTEGRAL discovery of a burst with associated radio emission from the magnetar SGR 1935+2154. *Astrophys. J. Lett.* **898**, L29 (2020).
15. Ridnaia, A. et al. A peculiar hard X-ray counterpart of a Galactic fast radio burst. *Nat. Astron.* https://doi.org/10.1038/s41550-020-01265-0 (2020).
16. Zhang, S.-N. et al. Insight-HXMT X-ray and hard X-ray detection of the double peaks of the fast radio burst from SGR 1935+2154. *Astron. Telegr.* 13696 (2020).
17. Locatelli, N. T. et al. The Northern Cross fast radio burst project—I. Overview and pilot observations at 408 MHz. *Mon. Not. R. Astron. Soc.* **494**, 1229–1236 (2020).
18. Pilia, M. et al. The lowest frequency fast radio bursts: Sardinia Radio Telescope detection of the periodic FRB 180916 at 328 MHz. *Astrophys. J. Lett.* **896**, L40 (2020).
19. Burgay, M. et al. Marginal detection of radio pulsations from the magnetar SGR 1935+2154 with the Medicina Northern Cross. *Astron. Telegr.* 13783 (2020).
20. Marcote, B. et al. A repeating fast radio burst source localized to a nearby galaxy. *Nature* **577**, 190–194 (2020).
21. Spitler, L. G. et al. A repeating fast radio burst. *Nature* **531**, 202–205 (2016).
22. CHIME/FRB Collaboration A second source of repeating fast radio bursts. *Nature* **566**, 235–238 (2019).
23. CHIME/FRB Collaboration CHIME/FRB discovery of eight new repeating fast radio burst sources. *Astrophys. J.* **885**, L24 (2019).
24. Scholz, P. et al. Simultaneous X-ray, gamma-ray, and radio observations of the repeating fast radio burst FRB 121102. *Astrophys. J.* **846**, 80 (2017).
25. Kirsten, F. et al. Simultaneous multi-frequency limits on radio emission at the time of a bright X-ray burst from SGR 1935+2154. *Astron. Telegr.* 13735 (2020).
26. Lyutikov, M. Radio emission from magnetars. *Astrophys. J.* **580**, L65–L68 (2002).
27. Kumar, P., Lu, W. & Bhattacharya, M. Fast radio burst source properties and curvature radiation model. *Mon. Not. R. Astron. Soc.* **468**, 2726–2739 (2017).
28. Lyubarsky, Y. A model for extragalactic radio bursts. *Mon. Not. R. Astron. Soc.* **442**, L9–L13 (2014).
29. Beloborodov, A. M. A flaring magnetar in FRB 121102? *Astrophys. J.* **843**, L26 (2017).
30. Palmer, D. M. et al. A giant γ-ray flare from the magnetar SGR 1806−20. *Nature* **434**, 1107–1109 (2005).
31. Hurley, K. et al. An exceptionally bright flare from SGR 1806−20 and the origins of short-duration γ-ray bursts. *Nature* **434**, 1098–1103 (2005).
32. Tendulkar, S. P., Kaspi, V. M. & Patel, C. Radio non-detection of the SGR 1806−20 giant flare and implications for fast radio bursts. *Astrophys. J.* **827**, 59 (2016).
33. Borghese, A. et al. X-ray monitoring of the active magnetar SGR 1935+2154. *Astron. Telegr.* 13720 (2020).
34. Airi, M. et al. Periodic activity from a fast radio burst source. *Nature* **582**, 351–355 (2020).
35. Tavani, M. et al. Gamma-ray and X-ray observations of the periodic-repeater FRB 180916 during active phases. *Astrophys. J. Lett.* **893**, L42 (2020).
36. Scholz, P. et al. Simultaneous X-ray and radio observations of the repeating fast radio burst FRB 180916.J0158+65. *Astrophys. J.* **901**, 165 (2020).
37. Metzger, B. D., Margalit, B. & Sironi, L. Fast radio bursts as synchrotron maser emission from decelerating relativistic blast waves. *Mon. Not. R. Astron. Soc.* **485**, 4091–4106 (2019).
38. Margalit, B., Beniamini, P., Sridhar, N. & Metzger, B. D. Implications of a fast radio burst from a Galactic magnetar. *Astrophys. J. Lett.* **899**, L27 (2020).
39. Casentini, C. et al. AGILE observations of two repeating fast radio bursts with low intrinsic dispersion measures. *Astrophys. J. Lett.* **890**, L32 (2020).
40. Katz, J. Are fast radio bursts made of neutron stars? *Mon. Not. R. Astron. Soc.* **494**, L64–L68 (2020).
41. Main, R. et al. Pulsar emission amplified and resolved by plasma lensing in an eclipsing binary. *Nature* **557**, 522–525 (2018).
42. Thompson, C. & Duncan, R. C. The soft gamma-ray repeaters as very strongly magnetized neutron stars—I. Radiative mechanisms for outbursts. *Mon. Not. R. Astron. Soc.* **275**, 255–300 (1995).
43. Hoshino, M. & Arons, J. Preferential positron heating and acceleration by synchrotron maser instabilities in relativistic positron–electron–proton plasmas. *Phys. Fluids B* **3**, 818–833 (1991).
44. Plotnikov, I. & Sironi, L. The synchrotron maser emission from relativistic shocks in fast radio bursts: 1D PIC simulations of cold pair plasmas. *Mon. Not. R. Astron. Soc.* **485**, 3816 (2019).
45. Kumar, P. & Lu, W. Radiation forces constrain the FRB mechanism. *Mon. Not. R. Astron. Soc.* **494**, 1217–1228 (2020).
46. Ridnaia, A. et al. Konus–Wind observation of hard X-ray counterpart of the radio burst from SGR 1935+2154. *GRB Coord. Netw.* 27669 (2020).
47. Connaughton, V. et al. Fermi GBM observations of LIGO gravitational-wave event GW 150914. *Astrophys. J. Lett.* **826**, L6 (2016).
48. Hill, J. E. et al. Readout modes and automated operation of the Swift X-ray Telescope. *Proc. SPIE* **5165**, https://doi.org/10.1117/12.505728 (2004).
49. Petroff, E. et al. FRBCAT: the fast radio burst catalogue. *Publ. Astron. Soc. Aust.* **33**, e045 (2016).
50. Prochaska, J. X. & Zheng, Y. Probing Galactic haloes with fast radio bursts. *Mon. Not. R. Astron. Soc.* **485**, 648–665 (2019).
51. McQuinn, M. Locating the "missing" baryons with extragalactic dispersion measure estimates. *Astrophys. J. Lett.* **780**, L33 (2014).
52. Cordes, J. M., Joseph, T., Lazio, W., NE2001. I. A new model for the galactic distribution of free electrons and its fluctuations. Preprint at https://arxiv.org/abs/astro-ph/0207156 (2002).
53. Tendulkar, S. P. et al. The host galaxy and redshift of the repeating fast radio burst FRB 121102. *Astrophys. J. Lett.* **834**, L7 (2017).
54. Bannister, K. W. et al. A single fast radio burst localized to a massive galaxy at cosmological distance. *Science* **365**, 565–570 (2019).
55. Prochaska, J. X. et al. The low density and magnetization of a massive galaxy halo exposed by a fast radio burst. *Science* **366**, 231–234 (2019).
56. Ravi, V. et al. A fast radio burst localized to a massive galaxy. *Nature* **572**, 352–354 (2019).
57. Macquart, J. P. et al. A census of baryons in the Universe from localized fast radio bursts. *Nature* **581**, 391–395 (2020).

Acknowledgements

AGILE is a space mission of the Italian Space Agency (ASI) developed and operated with the collaboration of INAF and INFN. The research was carried out with partial support by the ASI grants I/028/12/05 and ASI 2014-049-R.0. We acknowledge satellite operations at the ground station in Malindi (Kenya) and at AGILE mission operation centre in Fucino (Italy). We also acknowledge the scientific ground segment activities at the ASI Space Science Data Center. We thank the team of the Neil Gehrels Swift Observatory for assistance in supporting X-ray observations. We thank D. D. Frederiks for useful exchanges.

Author contributions

M. Tavani wrote the manuscript together with C.C., F.V. and A.U. C.P., F. Lucarelli and F.V. oversaw the AGILE satellite data flow and pipelines at the ASI Space Science Data Center. A.B., N.P., A. Argan, V.F. and L.B. contributed to the SW management and AGILE instrument pipelines. M.P. and S.P. contributed to the analysis of X-ray data. G. Bernardi, G. Bianchi, M.P., A. Magro, G.N., G. Pupillo and G.S. contributed to the analysis of radio data at the Northern Cross. Other authors belong to the whole AGILE team that contributed to supporting the writing of the manuscript and providing technical information and cross-check.

Competing interests

The authors declare no competing interests.

Additional information

Correspondence and requests for materials should be addressed to M.Tavani.

Peer review information *Nature Astronomy* thanks the anonymous reviewers for their contribution to the peer review of this work.